

# The Implications of Tropical Upper Tropospheric Momentum Flux Convergence to CRYSTAL

Matthew T. Boehm, NRC/NASA GSFC and David O'C. Starr, NASA GSFC

## Background

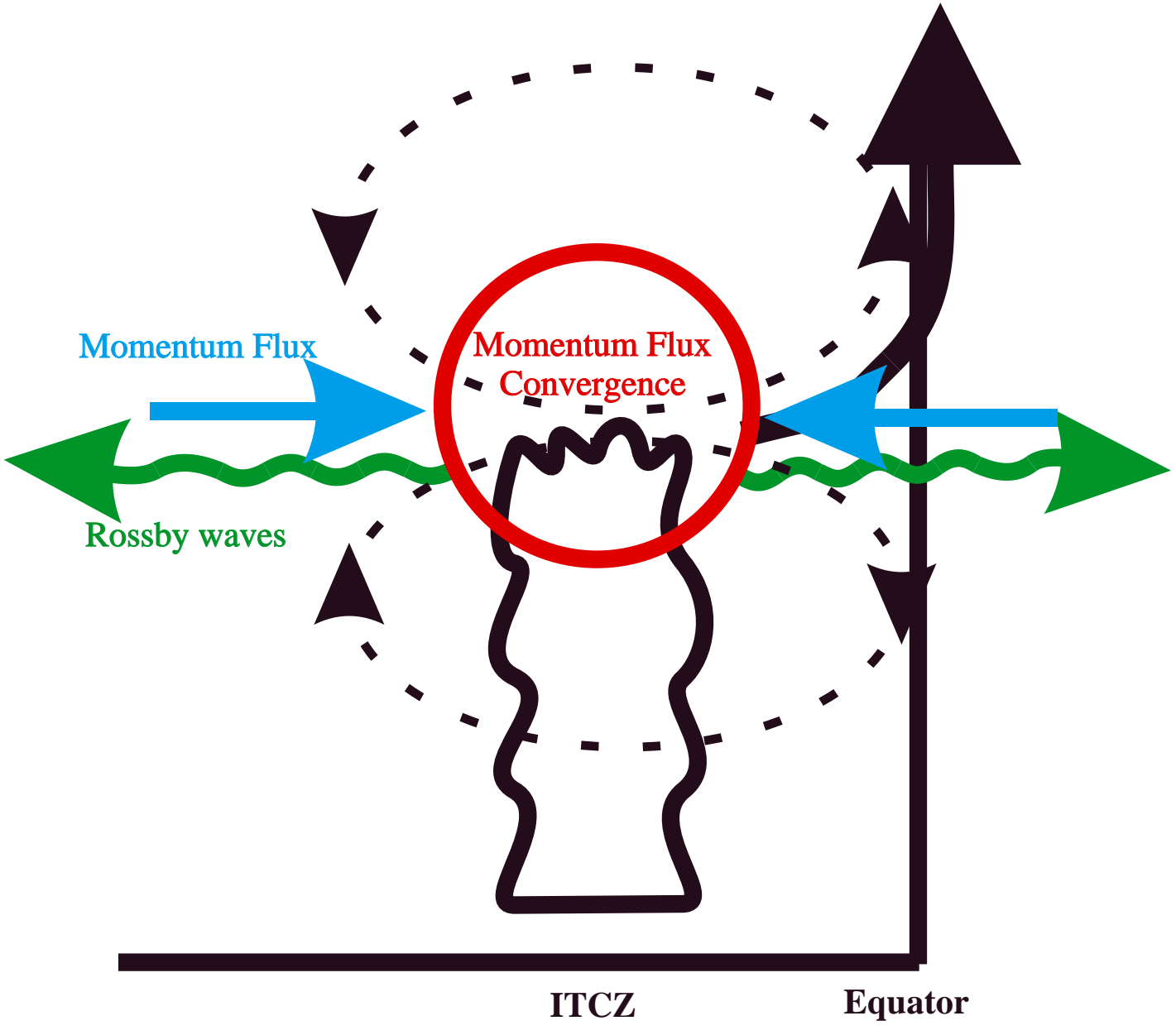
Analyzing 16 years of NCEP-NCAR reanalysis data, Lee (1999) showed that the net eddy momentum flux convergence is positive in the deep tropical upper troposphere, indicating that in this region Rossby wave momentum fluxes of tropical origin dominate those of mid-latitude origin. Furthermore, it was shown that the scales of the waves responsible for this convergence are consistent with those of ENSO and the MJO, suggesting that the eddy momentum flux convergence in the deep tropical upper troposphere is ultimately driven by convective heating.

Using model runs conducted with an axisymmetric global dynamical model, Boehm and Lee (2003) showed that this momentum flux convergence in the deep tropical upper troposphere is capable of driving a circulation that includes rising motion in the equatorial tropopause transition layer (TTL). It was suggested that this rising motion drives a portion of the Brewer-Dobson circulation, and also plays a role in transporting moisture vertically from where it is detrained from deep tropical convection to the cold-point tropopause, where sub-visible cirrus layers are often observed. The hypothesis presented by Boehm and Lee (2003) is illustrated in the figure below.

The purposes of this poster are to:

1) Take a closer look at the relationship between tropical convection and upper tropospheric momentum flux convergence

2) Provide a large-scale dynamical context for CRYSTAL-FACE and input to decisions regarding a future CRYSTAL mission



Summary of Boehm and Lee (2003) hypothesis

1) The spatial and temporal variability of tropical convective heating generates Rossby waves that propagate poleward.

2) These waves lead to an equatorward meridional flux of zonal momentum.

3) This momentum flux converges in the tropical upper troposphere near the ITCZ.

4) This convergence leads to zonal wind acceleration, tending to destroy thermal wind balance.

5) Circulations develop to maintain thermal wind balance (dotted lines and thick arrow).

## Convergence Calculations

We have developed and implemented a new method for calculating momentum flux convergence from reanalysis data. This method builds on the work of Gu and Zhang (2001), who combined wavelet analysis in longitude with Fourier analysis in time to study the longitudinal dependence of waves in outgoing longwave radiation data. The steps in this analysis are given below and illustrated in the figure at right.

1) Remove annual cycle from NCEP-NCAR reanalysis zonal (u) and meridional (v) wind fields

2) Extract a time-longitude cross-section from this data

3) Apply wavelet analysis in longitude to this cross-section, adding a third dimension of wavenumber (k)

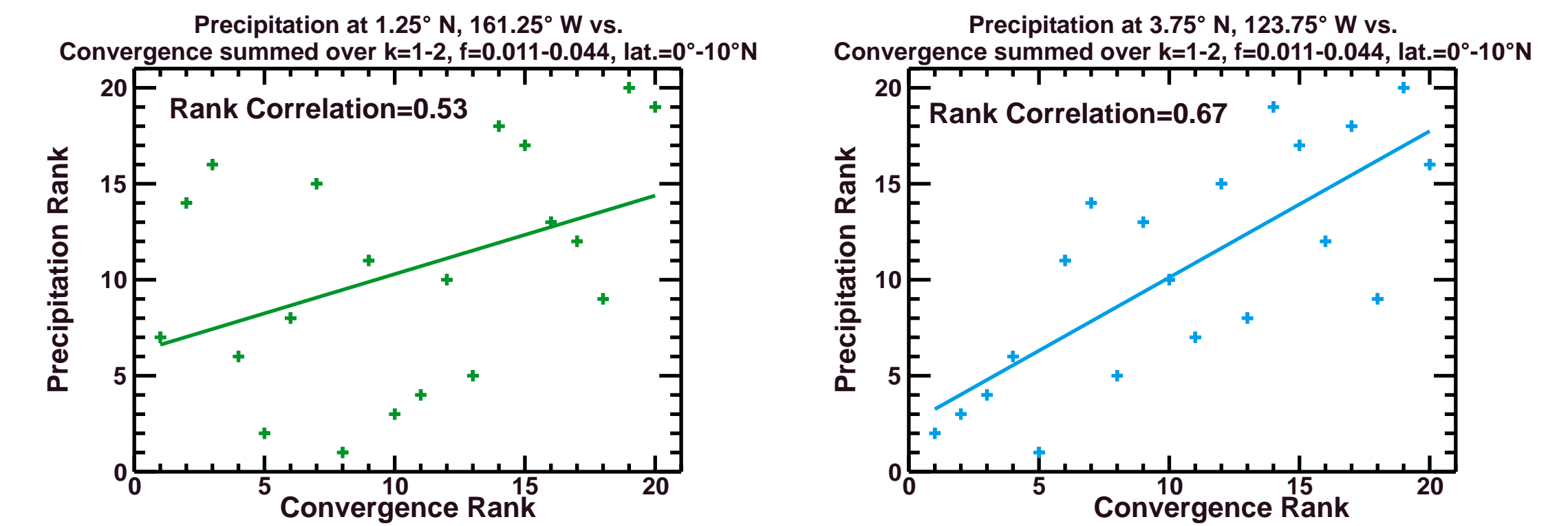
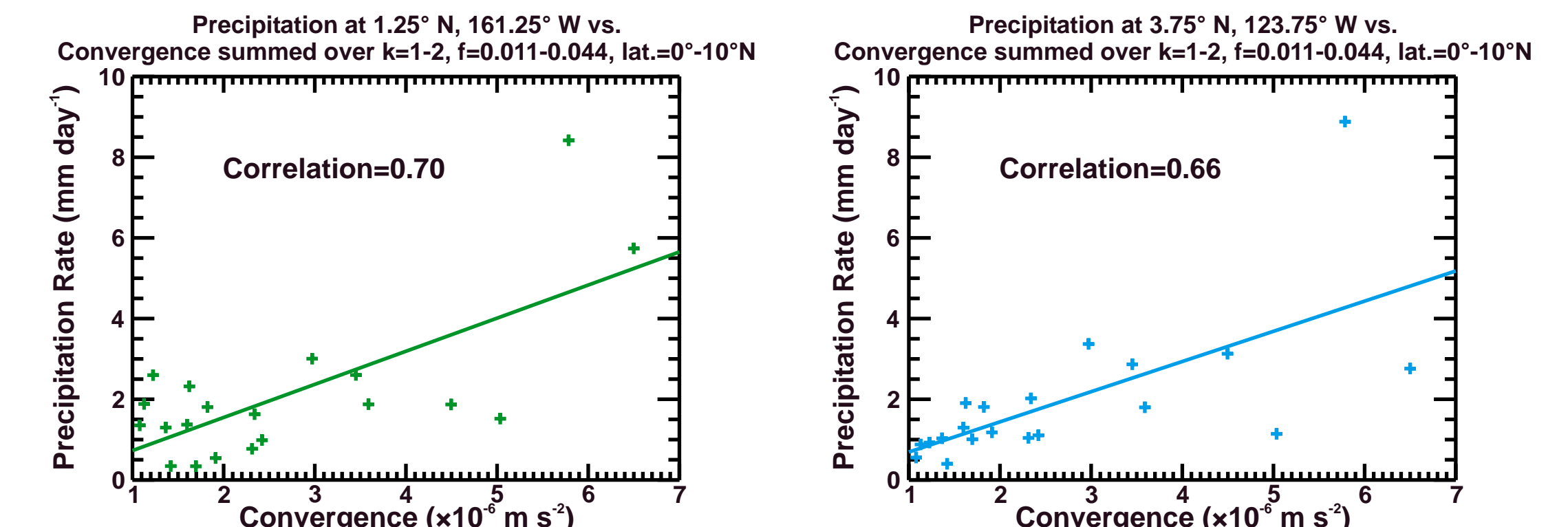
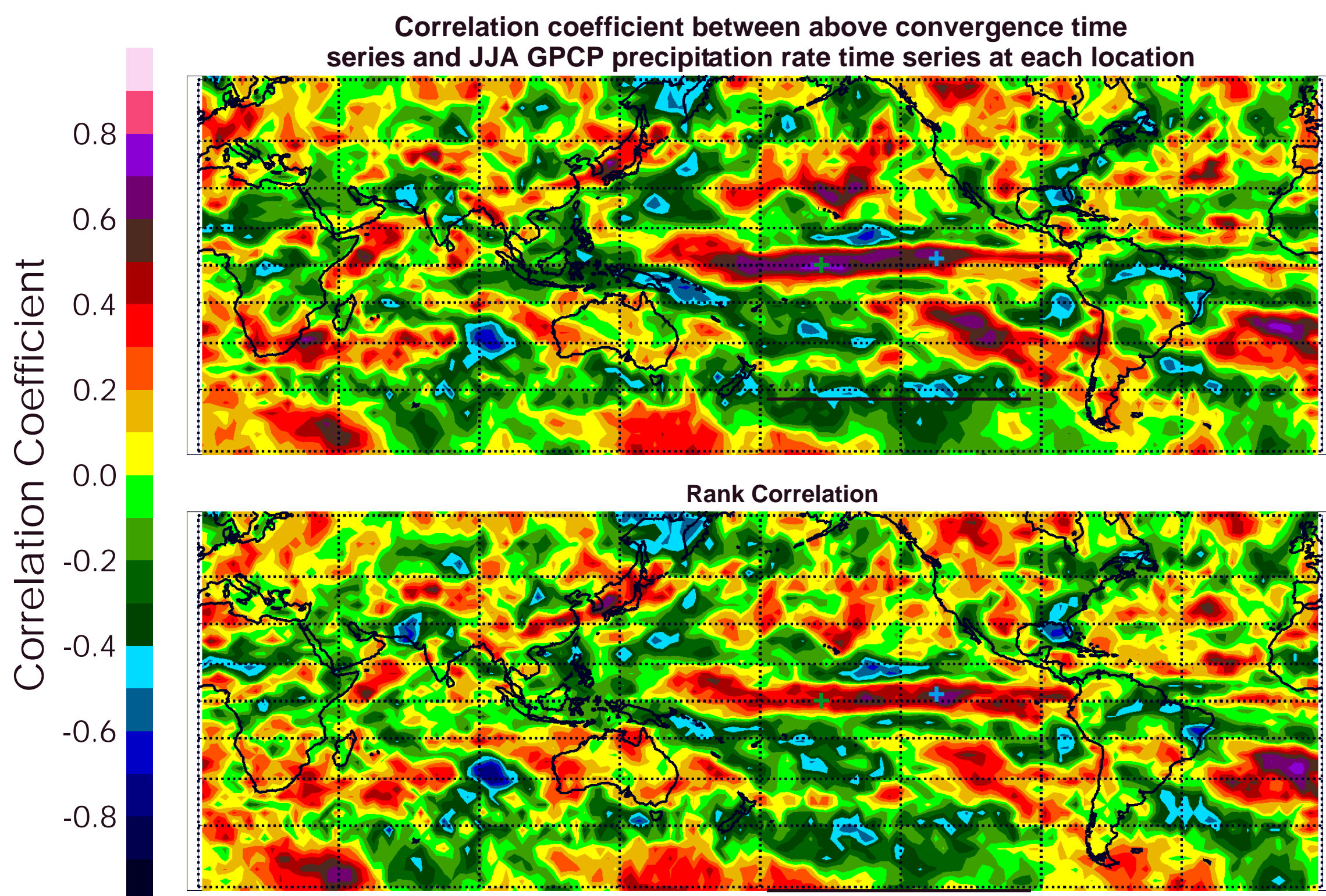
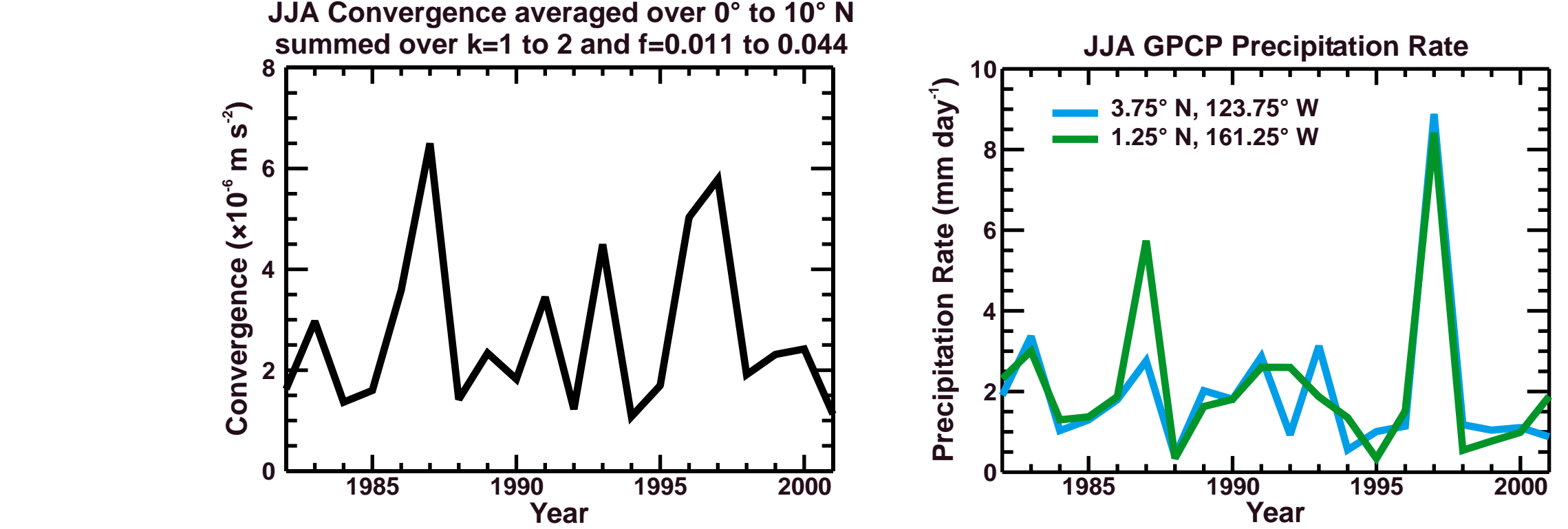
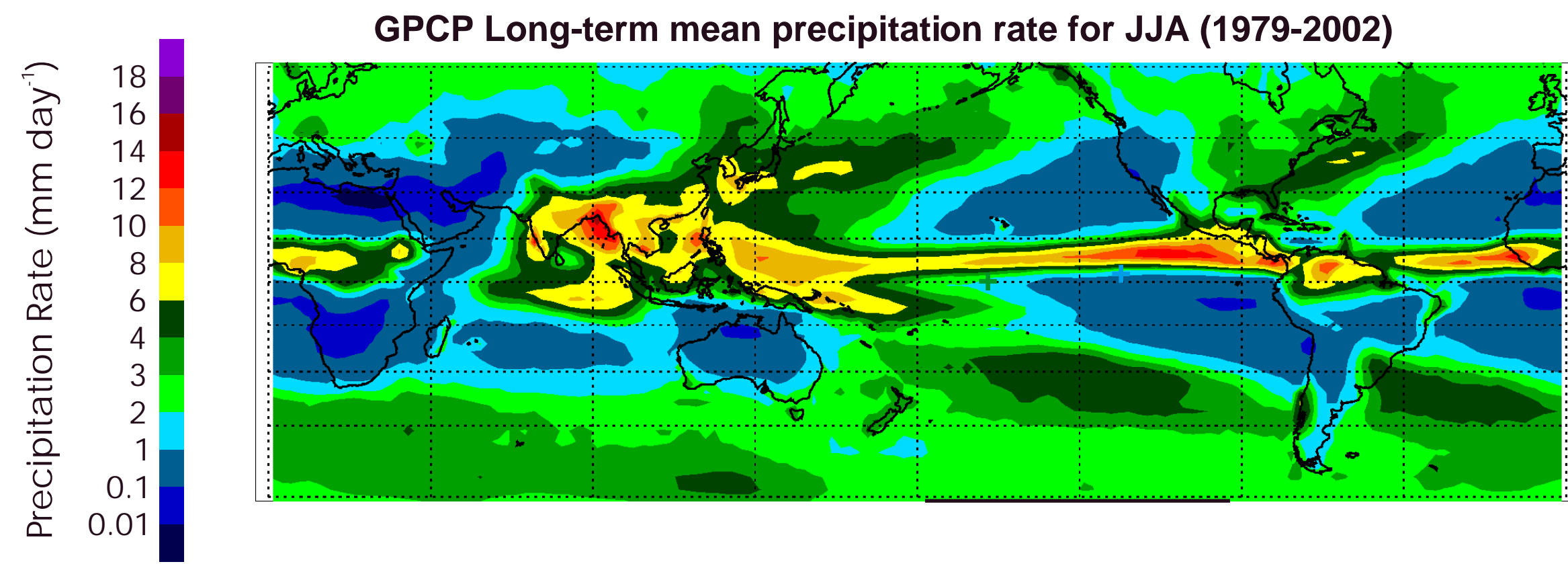
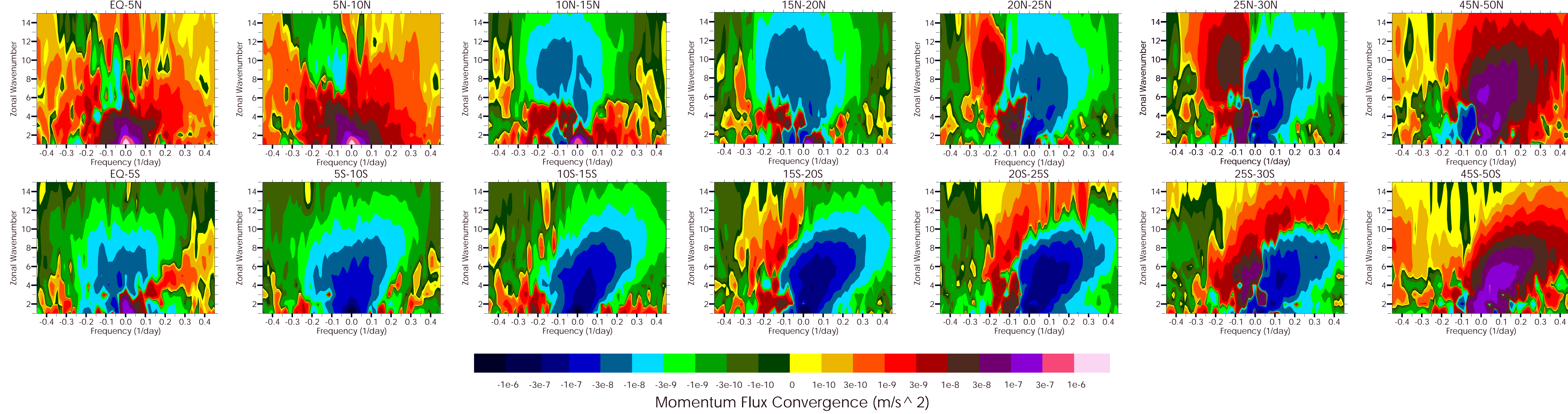
4) Take the Fourier transform of the wavelet analysis, converting the time dimension to frequency (f)

5) Momentum flux is then calculated using  $uv(k, f, \lambda) = \frac{2 \text{Re} \{ \hat{U}(k, f, \lambda) \hat{V}^*(k, f, \lambda) \}}{(n \text{lon})(\text{cor})}$

6) Performing these calculations at all desired latitudes, pressure levels, and time periods yields:

$$uv(k, f, \lambda, P, t)$$

7) Finally, meridional momentum flux convergence,  $-\text{div}_y v$ , is calculated using a centered differencing scheme.



## The Convection-Convergence Connection

The zonal mean momentum flux convergence figures shown above reveal that momentum flux convergence is prevalent in the tropical upper troposphere. Here we examine the relationship between this convergence and tropical convection, using data from the Global Precipitation Climatology Project (GPCP) as a proxy for tropical convection.

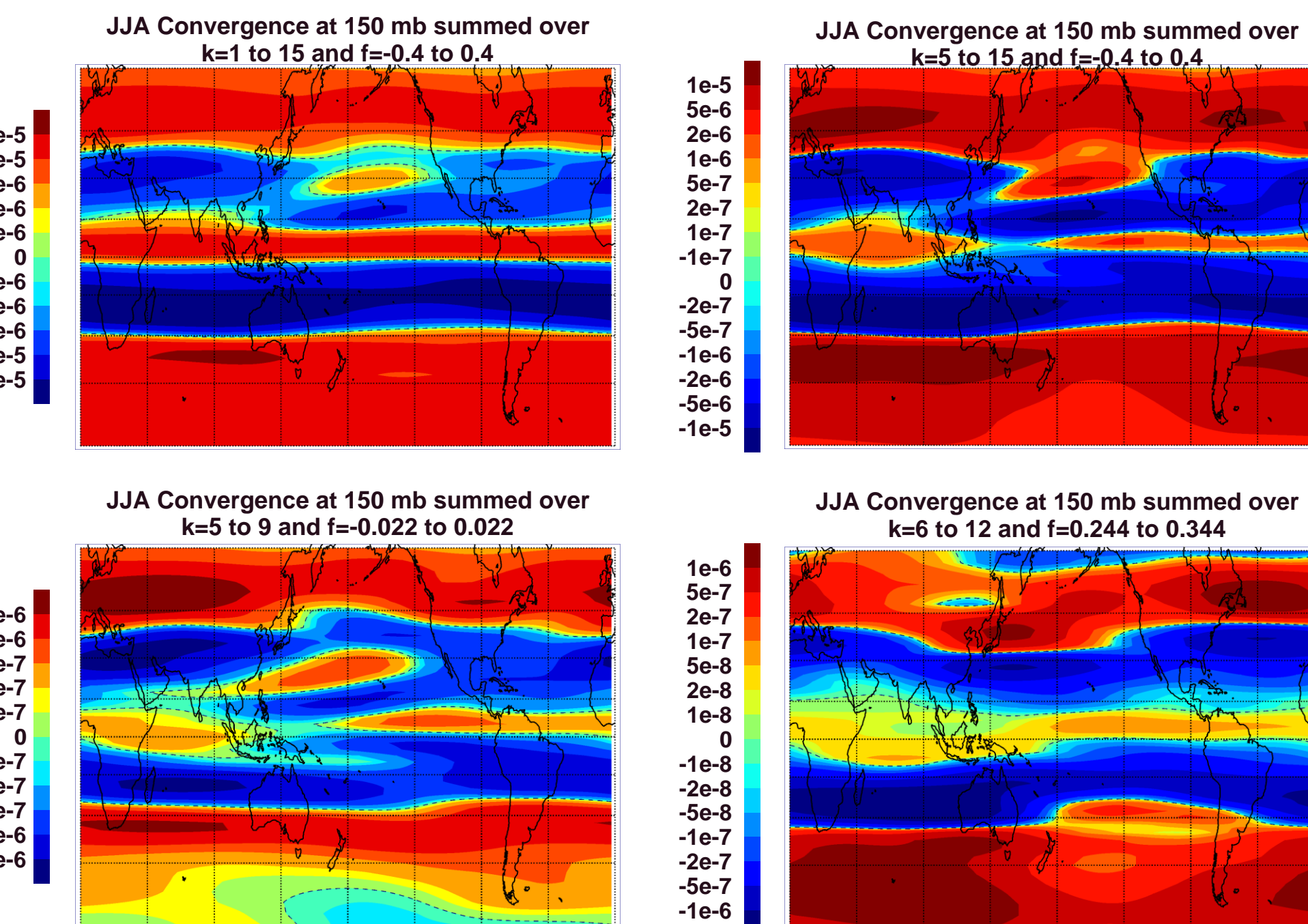
The time series at far left shows the momentum flux convergence at 150 mb for JJA summed over zonal wavenumbers 1-2 and frequencies 0.011-0.044 day^-1 (periods 23-90 days) and averaged over latitudes 0°-10°N. These ranges were chosen since they correspond to the maximum tropical convergence values in the zonal mean figures, and also to the characteristic ranges of the MJO which Lee (1999) showed is connected to upper tropical momentum flux convergence.

The lower left figures are maps of the correlation and rank correlation coefficients between the convergence time series just described and the 20-year time series of GPCP JJA precipitation at each point. Large positive values are found across much of the Pacific Ocean just north of the equator, suggesting that convection in the ITCZ (see precipitation figure at top left) is closely connected to momentum flux convergence at MJO wavenumbers and frequencies.

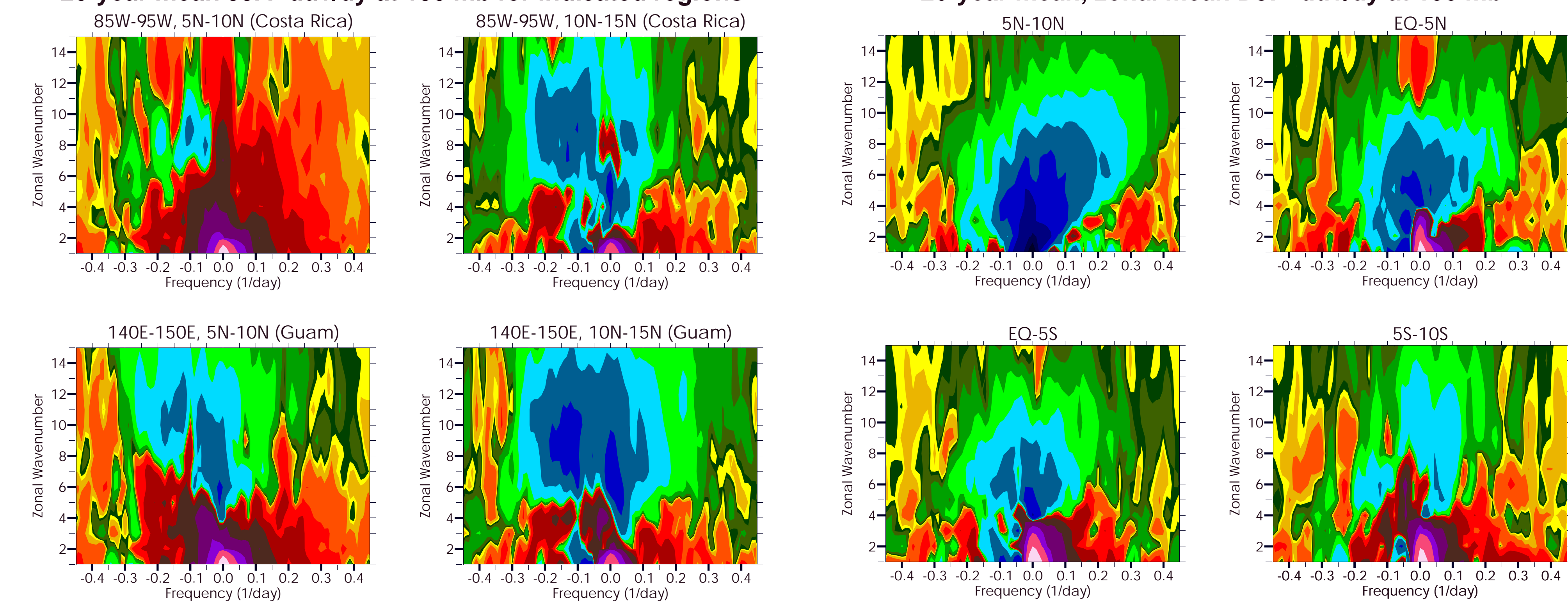
To more closely examine this connection, we show at left precipitation time series at a couple of points, indicated by blue and green '+'s in the maps at left, in the central Pacific high correlation region. As expected based on the relatively high correlation values at these points, the convergence and precipitation time series generally track each other. The scatter plots of precipitation vs. convergence presented at lower left further illustrate this. The rank scatter plots reveal that the connection between convection and convergence is stronger at the blue '+' than at the green '+', even though the standard correlation coefficient is higher at the green '+' (0.70 vs. 0.66 at the blue '+').

The figures below show maps of JJA momentum flux convergence at 150 mb summed over different ranges of wavenumber and frequency. The general features of each map are similar and are consistent with the zonal mean convergence plots presented elsewhere, with mid-latitude convergence, sub-tropical divergence, and a relatively narrow band of deep tropical convergence at the latitude of the ITCZ. The frequency and wavenumber range for the upper left panel corresponds to nearly the entire range shown in the zonal mean convergence plots. Over this range, the deep tropical convergence is nearly constant with longitude because the convergence is dominated by very low wavenumbers, for which longitudinal variability can not be shown. Longitudinal variability in the deep tropics is evident in the remaining three panels, since they are confined to higher wavenumbers. In the upper right map, convergence is summed over the same range as the upper left map, but the wavenumber range is decreased to 5-15. The lower left panel shows convergence summed over both eastward and westward propagating waves with very low frequencies (corresponding to periods longer than 45 days) and the wavenumber range 5-9. Finally, the lower right map shows convergence due to eastward propagating, higher frequency (periods 3-4 days) waves for wavenumber 6-12. For each of these three ranges, the maximum deep tropical convergence is located in the central to eastern Pacific, slightly to the west of the eastern Pacific precipitation maximum, with a secondary maximum in the Indian Ocean slightly to the west of the precipitation maximum in the central Indian Ocean.

Another interesting feature in these figures is the southwest-to-northeast oriented region of convergence surrounded by divergence in the central North Pacific Ocean. This feature may be related to tropical storms, as a plot (not shown) of convergence as a function of frequency and wavenumber for this region shows a peak for westward propagating periods 5-20 days at wavenumbers 8-12.



## 20-year mean JJA -div/dy at 150 mb for indicated regions



## Implications to CRYSTAL

### CRYSTAL-FACE:

-Momentum flux convergence characteristics are very different at Florida latitudes (25°N-30°N) than at ITCZ latitudes (5°N-10°N)

-Large-scale wave forcing is not expected with Florida storms since they are typically generated by local forcing over a small region.

### CRYSTAL-NEXT (Recommendations for the next CRYSTAL experiment)

#### Location (Costa Rica vs. Guam in JJA)

-To study tropopause cirrus and large-scale upwelling in the tropopause layer at either location, it is desirable to fly as far south as possible, since the convective signal in convergence is much more prominent in 5°N-10°N band than in 10°N-15°N band; and the maximum large-scale rising motion is expected equatorward of the convergence maximum.

-As shown in the figures above, momentum flux convergence is substantially stronger and occurs over a broader range of frequency and wavenumber near Costa Rica (85°W-95°W) than near Guam (140°E-150°E). This is likely due to both stronger convection at Costa Rica and more impact of momentum flux divergence due to mid-latitude waves at Guam.

-Recommendation Costa Rica.

#### Season (JJA vs. DJF)

-The tropical convergence maximum shifts from north of the equator in JJA to south of the equator in DJF in association with the shift in the ITCZ. This shift is visible in the convergence maps below and the plots of zonal mean DJF convergence as a function of frequency and wavenumber above. Costa Rica and Guam are not recommended locations during DJF.

-Tropical convergence is much more confined to low wavenumbers in DJF. This may be due to the stronger impact of divergence due to breaking mid-latitude waves in northern winter outwighing convergence due to waves generated in the tropics.

-Recommendation JJA, due to easier access to the region of maximum convergence and reduced impact from mid-latitudes.

